Acta Mechanica 100, 105–114 (1993)

ACTA MECHANICA

Analysis of shear bands in a dynamically loaded viscoplastic cylinder containing two rigid inclusions

R. C. Batra and **X.-T. Zhang,** Rolla, Missouri

(Received April 14, 1992)

Summary. We study plane strain thermomechanical deformations of a hollow circular cylinder containing two rigid non-heat-conducting ellipsoidal inclusions placed on a radial line symmetrically with respect to the center. These inclusions can be viewed as precipitates or second phase particles in an alloy. The material of the cylinder is presumed to exhibit thermal softening, but strain and strain-rate hardening. The impact load applied on the inner surface of the cylinder is modeled by prescribing a radial velocity and zero tangential tractions at material particles situated on the inner surface. Rigid body motion of the inclusion is considered and no slip condition between the inclusion and the cylinder material is imposed.

It is found that shear bands initiate from points adjacent to inclusion tips near the inner surface of the cylinder and propagate toward this surface. At inclusion tips near the outer surface of the cylinder, the maximum principal logarithmic strain and the temperature are high and the effective stress is low, but severe deformations there do not propagate outward.

1 Introduction and problem formulation

In a previous paper [1] we studied the problem of the initiation and growth of shear bands in a dynamically loaded and thermally softening viscoplastic cylinder undergoing plane strain deformations. Two ellipsoidal voids placed on a radial line symmetrically with respect to the center were taken to be nucleation sites for the bands. Here we study the same problem, except that the voids are replaced by rigid inclusions. Zhu and Batra [2] have investigated the initiation of shear bands from inclusion tips embedded at the centroid of a square cross-section. However, the inclusion was stationary because of the symmetry of the deformations. Here each inclusion can move in the radial direction; we account for its inertia, and compare computed results with those obtained when the inclusions are replaced by voids. This comparison should reveal which one of the two is a stronger defect in the sense that it causes the shear band to initiate sooner.

We note that much of the literature on shear bands is given in the two papers [1], [2] cited above, and refer the reader to these papers for references related to this work. The study of shear bands is important, since they act as precursors to shear fractures, and once a shear band has formed subsequent deformations of the body occur within this narrow region with the rest of the body undergoing very little deformations.

The geometric configuration for the problem studied and the finite element mesh used to analyze it are shown in [1, Figs. 1 and 2]. Here the void of [1] is replaced by an identical non-heat-conducting rigid inclusion. We refer the reader to [1] for the governing equations, boundary conditions, constitutive relations, and a brief description of the method used to solve the problem. Whereas the void surface in [1] was taken to be thermally insulated and traction free, here we require that displacements and surface tractions are continuous across the cylinder/inclusion interface. Because of the presumed symmetry of deformations about the horizontal and vertical centroidal axes, the rigid inclusion can move only horizontally and the relevant equation of motion is

$$m\dot{v}_1{}^r = F_1, \qquad F_1 = -\int \sigma_{1j} n_j \, ds, \tag{1}$$

where the line integration is over the inclusion/cylinder material interface, n_j is an outward unit normal to this surface and pointing into the inclusion, σ_{ij} is the Cauchy stress tensor evaluated at cylinder particles abutting the inclusion, the integration path is traversed so that the cylinder material lies to our left, $v_1{}^r$ is the velocity of the rigid inclusion in x_1-direction, and m is the mass of the inclusion in a cylinder of unit length.

Here we also account for the work-hardening of the cylinder material and employ the following constitutive relation to describe its thermomechanical response.

$$\begin{aligned}
&\sigma_{ij} = -p(\varrho)\,\delta_{ij} - \alpha K(\theta - \theta_0)\,\delta_{ij} + 2\mu D_{ij},\\
&2\mu = \frac{\sigma_0}{\sqrt{3}\,I}\,(1 + bI)^m\,(1 - \nu(\theta - \theta_0))\left(1 + \frac{\psi}{\psi_0}\right)^n, \qquad p(\varrho) = B\left(\frac{\varrho}{\varrho_0} - 1\right),\\
&\dot{\psi} = 2\mu \bar{D}_{ij}\bar{D}_{ij} \bigg/ \left(1 + \frac{\psi}{\psi_0}\right)^n, \qquad 2I^2 = \bar{D}_{ij}\bar{D}_{ij}, \qquad \bar{D}_{ij} = D_{ij} - \frac{1}{3}\,D_{kk}\delta_{ij},
\end{aligned} \tag{2}$$

where σ_{ij} is the Cauchy stress tensor, α the coefficient of thermal expansion, K the bulk modulus, θ the present temperature of a material particle, θ_0 its initial temperature, D_{ij} is the strain-rate tensor, σ_0 the yield stress in a quasistatic simple tension or compression test, ν the coefficient of thermal softening, and ψ is an internal variable used here to describe the work hardening of the material. The material parameters b and m characterize the strain-rate hardening of the material, and ψ_0 and n its work hardening.

2 Results and discussion

The material and geometric parameters are assigned values as in [1], and we set

$$\begin{aligned}
&K = 168\ \text{GPa}, \qquad \varrho_i = 2\varrho_r, \qquad \psi_0 = 0.017,\\
&n = 0.1, \qquad \alpha = 10.8 \times 10^{-6}\,{}^\circ\text{C}^{-1}, \qquad \theta_0 = 25\,{}^\circ\text{C},
\end{aligned} \tag{3}$$

where ϱ_i is the mass density of the inclusion.

Results presented below are in terms of nondimensional variables defined in [1]. Figure 1 depicts the variation of the rigid inclusion velocity with time. Because of the dissipation of energy due to plastic working and heat conduction, the speed of the inclusion gradually dies out. The peak speed of the inclusion depends upon its mass density and the values of parameters for the cylinder material. The evolution of the maximum principal logarithmic strain ε, the temperature, and the effective stress s_e, at four points P, Q, R, and S located on the horizontal axis is plotted in Figs. 2a, b, and c, respectively. Points Q and R represent cylinder particles adjoining, respectively, the left and right tips of the inclusion, and P and S are situated on the inner and outer surfaces of the hollow cylinder. The effective stress s_e and the maximum principal logarithmic

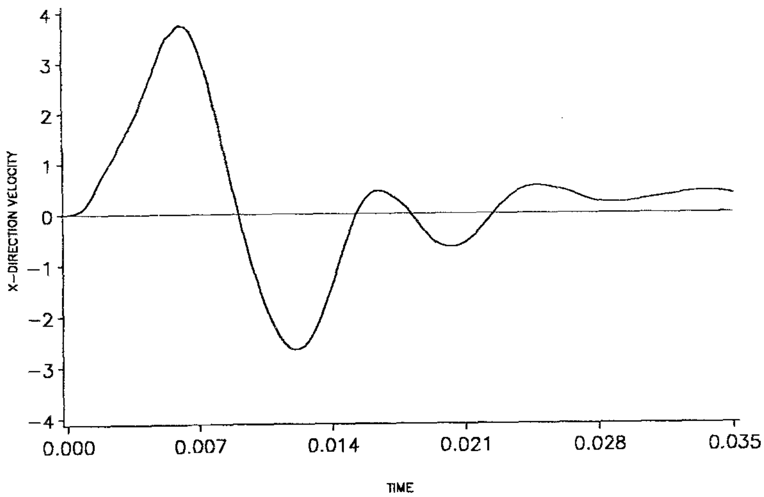

Fig. 1. Variation of the x_1-velocity of the rigid inclusion with time

strain ε are defined as

$$s_e = \left(\frac{1}{2}\operatorname{tr} ss^T\right)^{1/2} = \frac{1}{\sqrt{3}}(1 + bI)^m \left(1 - \nu(\theta - \theta_0)\right)\left(1 + \frac{\psi}{\psi_0}\right)^n, \tag{4.1}$$

$$\varepsilon = \ln \lambda_1, \tag{4.2}$$

where $\lambda_1{}^2$ is the maximum eigenvalue of the left or right Cauchy-Green tensor and s is the deviatoric stress tensor. Because of the oscillatory motion of the rigid inclusion, values of ε at points Q and R increase gradually, attain a local maximum at time $t = 0.0085$, and then fall off slowly. Once the inclusion has essentially come to rest, ε at points Q and R increases. The values of ε at points P and S increase monotonically , but are quite small relative to the peak values of ε at points Q and R. For $\varepsilon = 0.3$, the stretch equals 1.35, and the nominal strain 0.25. The temperature rise at points P and S is minuscule as compared to that at points Q and R. The temperature of each of these four points increases monotonically; the temperature of point Q on the left inclusion tip is always higher than that of point R on the right inclusion tip. The effective stress s_e at points Q and R increases first because of the strain and strain-rate hardening of the material, but then decreases essentially monotonically because this hardening is exceeded by the softening of the material due to its being heated up. The peak values of s_e at points Q and R occur at different times, even though ε attains the maximum value there at about the same instant. It is due to the different values of the temperature and possibly strain-rates. In our previous studies [1]–[3] of shear banding in one and two-dimensional problems, values of ε and θ at the point of the initiation of the band increased monotonically and in consonance with each other throughout the localization process. However, in the present problem, because of the oscillatory motion of the rigid inclusion, the point where ε assumes maximum values at any instant of time keeps on changing.

Figure 3 depicts the contours of the maximum principal logarithmic strain at $t = 0.01$, 0.02, and $t = 0.035$, and of the temperature at time $t = 0.035$. We note that the subroutine used to plot these contours interpolates data at numerous points in the domain from that supplied at either nodal points or quadrature points of the elements. The temperature contours suggest that shear bands initiate from points near both inclusion tips. However, the contours of the maximum

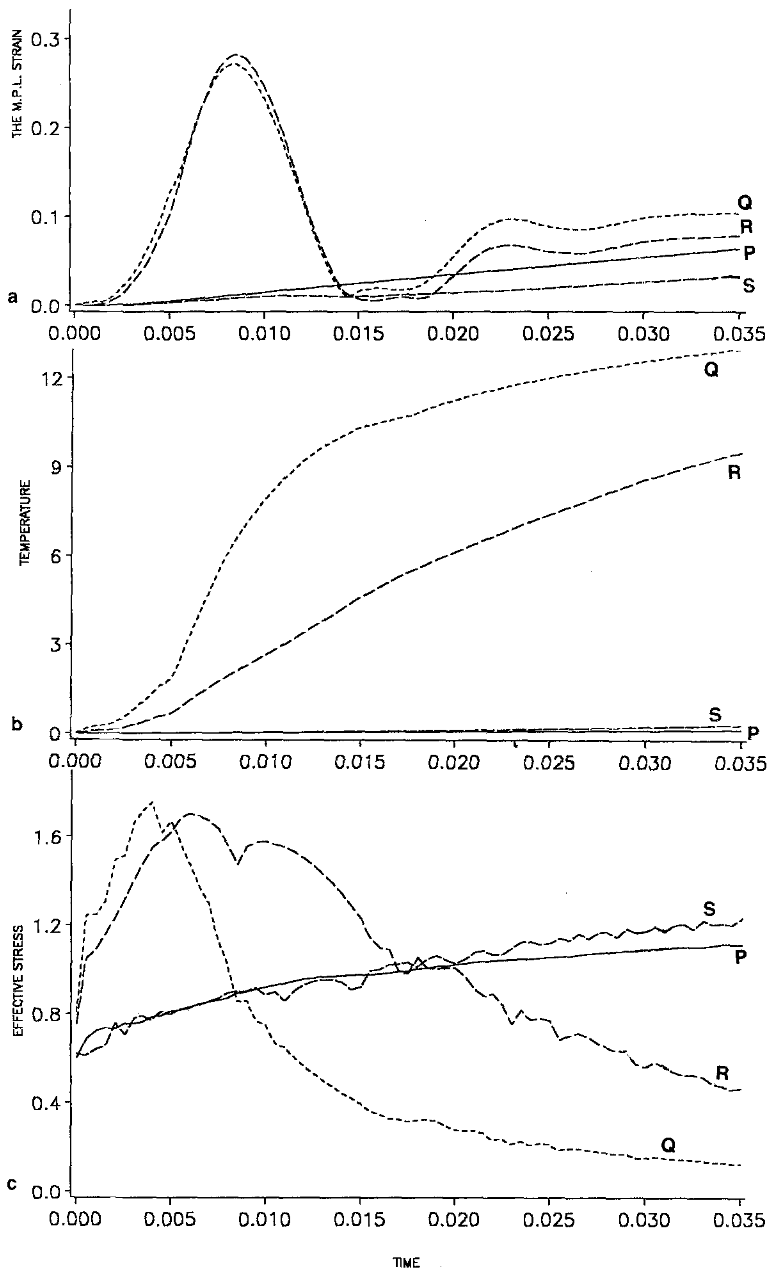

Fig. 2. Evolution of the maximum principal logarithmic strain, temperature, and the effective stress at points P, Q, R, and S. Coordinates of these points in the stress-free reference configuration are P (0.5016, 0.0018), Q (0.7193, 0.0033), R (0.7764, 0.0035), and S (0.9984, 0.0027).

principal logarithmic strain indicate that initially severe deformations occur at points near both inclusion tips, but those at points near the right inclusion tip subside and those at points adjacent to the left inclusion tip become more intense and propagate toward the inner surface. This is confirmed by a plot, given in Fig. 4, of the deformed mesh embedded in a small region surrounding the inclusion. We note that this mesh was not used to solve the problem. Coordinates of node points for this mesh in reference and present configurations were obtained from the coordinates of node points in the mesh in the unstressed reference configuration and the

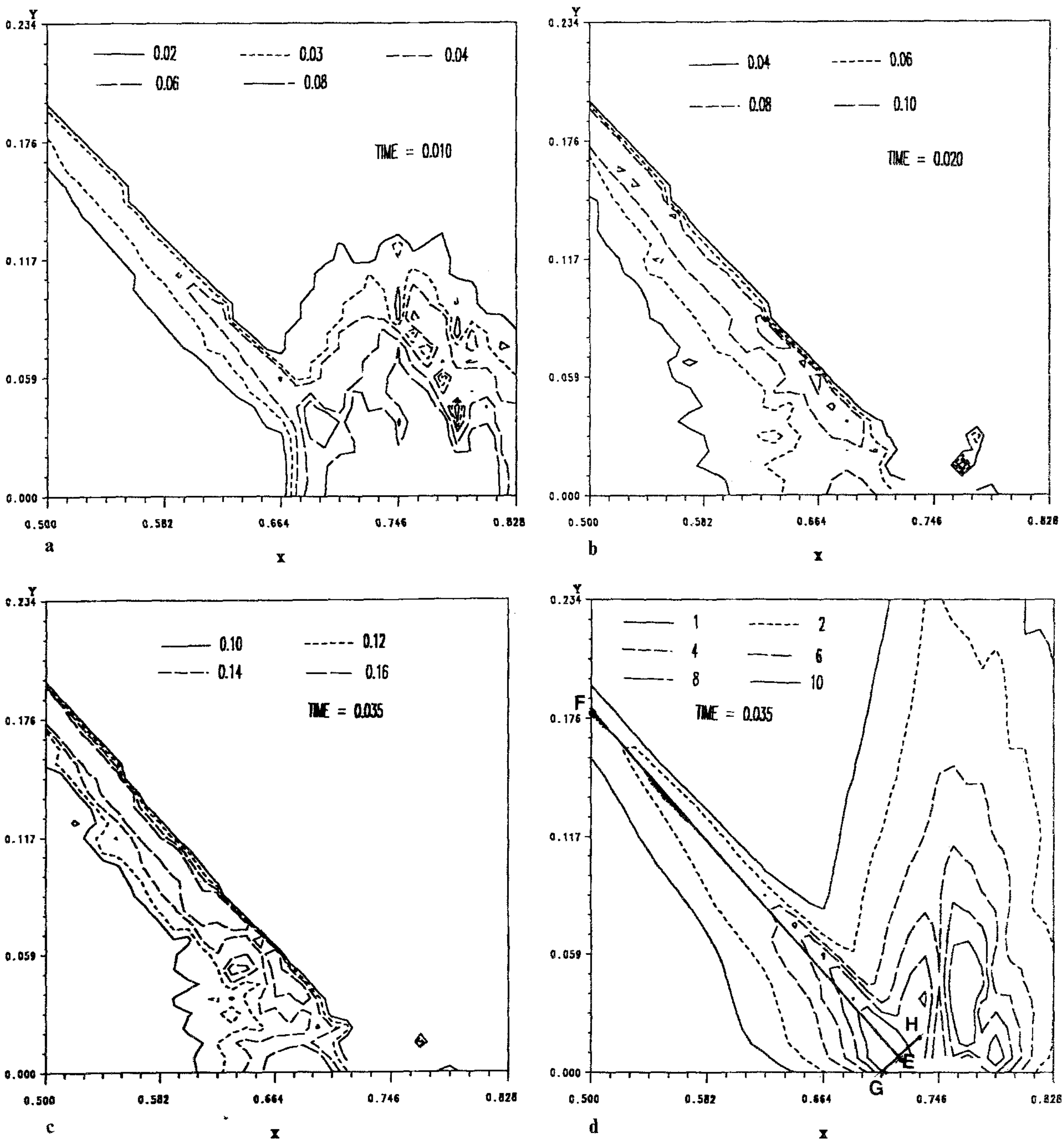

Fig. 3a–d. Contours of the maximum principal logarithmic strain at three different times and of the temperature at $t = 0.035$

solution of the problem. In our earlier investigation [1] involving a void where we have inclusion now, we found that a small region near the right void tip also deformed severely, but these intense deformations did not propagate to distant points. The presently computed results suggest that the temperature rise and stress drop at a point in a two-dimensional problem may make the material there unstable, but this instability need not propagate outward from that point. Perhaps factors such as the rates of temperature rise and of stress drop, and the state of deformation of the material surrounding the point where the stress drop occurs are equally important, too.

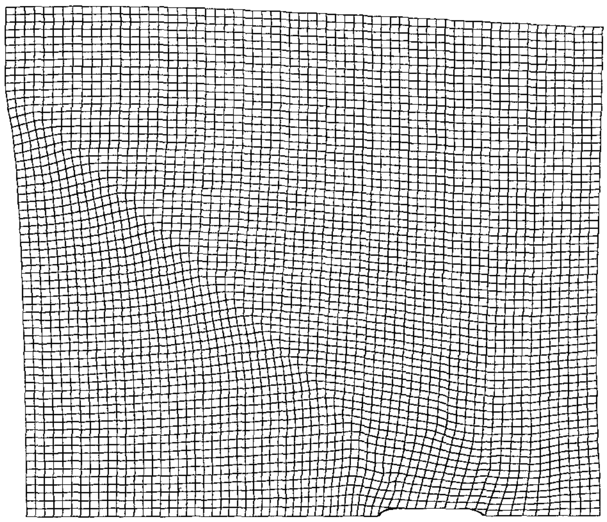

Fig. 4. Deformed mesh embedded in a small region surrounding the rigid inclusion

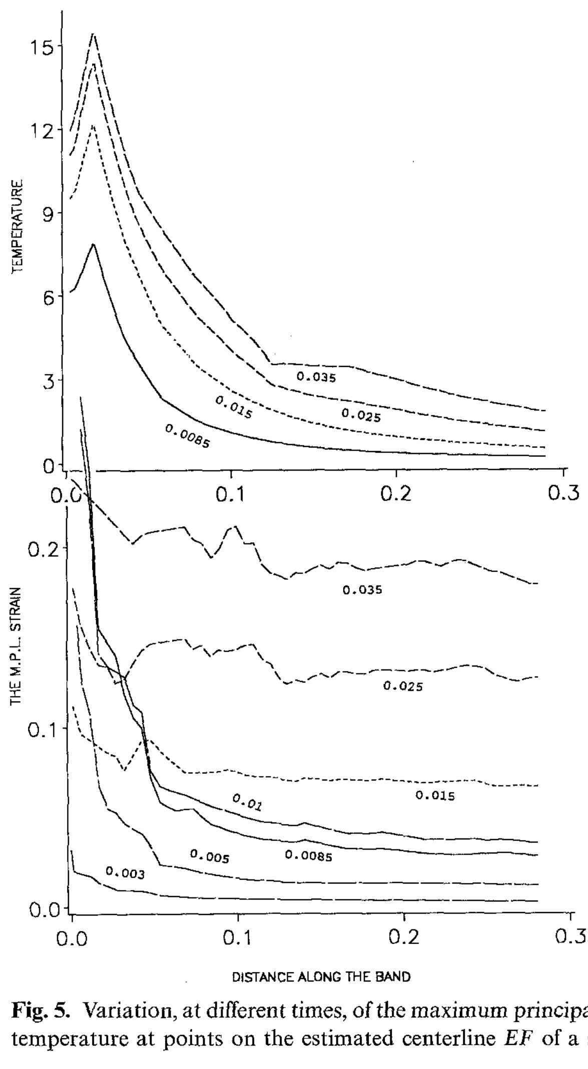

Fig. 5. Variation, at different times, of the maximum principal logarithmic strain within the band, and of the temperature at points on the estimated centerline EF of a shear band

From the contours of ε and the deformed mesh, we estimate the centerline of the shear band to be the line EF shown in Fig. 3d. The variation of the temperature at points on EF and of the maximum principal logarithmic strain within the band for different values of time is shown in Fig. 5. The values of the maximum principal logarithmic strain were obtained by computing its values at several points on a line perpendicular to EF, finding the largest of these values, and assigning that value to the point of intersection of the transverse line with EF. We note that ε varies noticeably at points on the transverse line as depicted below in Fig. 6. As oscillations of the rigid inclusion diminish, the strain within the band tends to become uniform. Whereas the maximum strain occurs at a point close to E, the peak temperature occurs at a point on line EF that is slightly away from E. The distribution, at different times, of the temperature and the maximum principal logarithmic strain at points on line GH (cf. Fig. 3d for the location of line GH) perpendicular to EF is shown in Fig. 6. The abscissa is the distance of a point from G along the line GH. Whereas the temperature at material points on line GH changes gradually as one

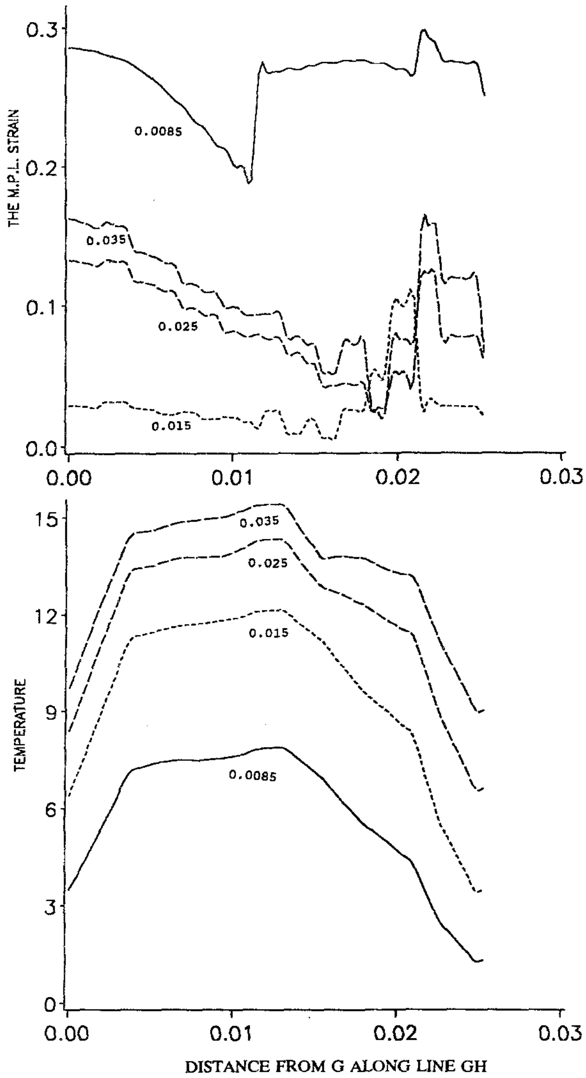

Fig. 6. Variation, at different times, of the maximum principal logarithmic strain and the temperature across the shear band

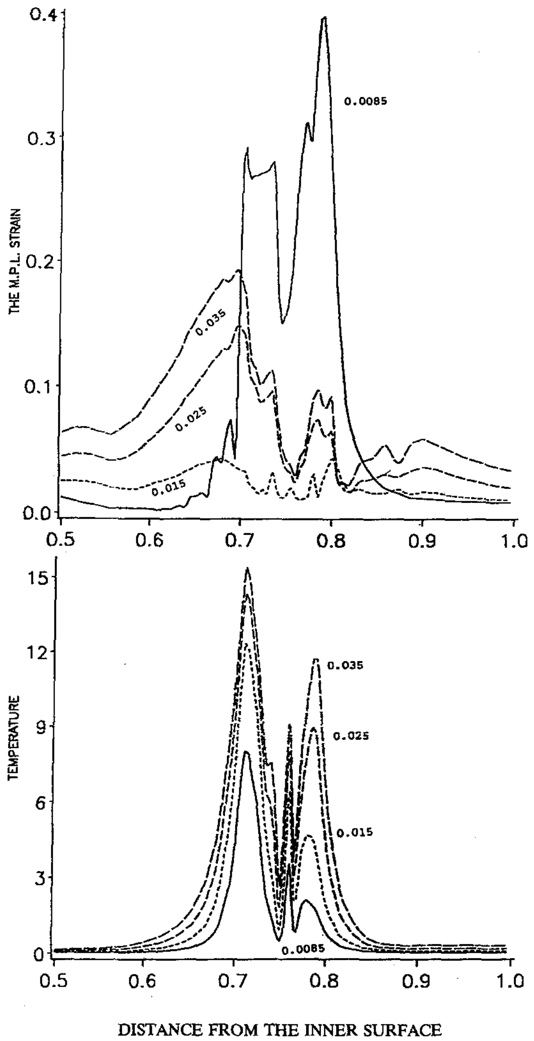

Fig. 7. Variation, at different times, of the maximum principal logarithmic strain and the temperature on a horizontal line tangent to the inclusion tip

moves along the line *GH*, the strain does not. The computations were stopped when a material point had melted. The melting of one material point does not imply the failure of the body since the neighboring material holds it together. It seems that the use of an adaptively refined mesh would probably result in sharper gradients of temperature and strain along line *GH*.

The distribution of the maximum principal logarithmic strain and temperature at points on a horizontal line *VW* tangent to the inclusion is exhibited in Fig. 7. The abscissa in the figure equals the distance from the inner surface of the cylinder (i.e., point *V*) of a point on line *VW*. Oscillations of the rigid inclusion affect noticeably the location of the point where peak values of ε occur. The strain and temperature at points near the left inclusion tip are higher than those at points near the right inclusion tip.

Figure 8 depicts how the average pressure

$$p = -\frac{2}{\pi} \int_{0}^{\pi/2} \sigma_{rr}(r_i, \theta)\, d\theta \tag{5}$$

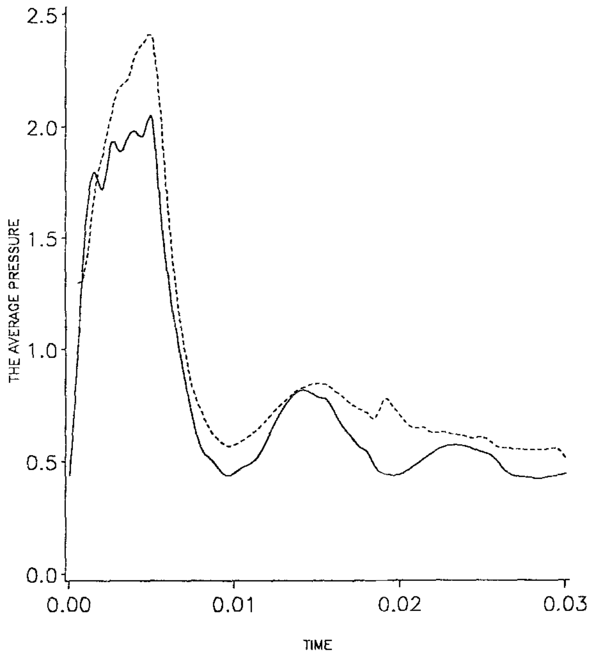

Fig. 8. Variation with time of the average pressure acting on the inner surface of the cylinder. —— inclusion ------ void

on the inner surface of the cylinder varies with time. In Eq. (5), r_i equals the inner radius of the deformed cylinder. The solid curve corresponds to the case of the rigid inclusion and the broken one to that of an identical void. Note that essential boundary conditions are prescribed on the inner surface, and the outer surface is traction free. If the shear band is assumed to initiate when the pressure on the inner surface drops precipitously, then the rigid inclusion causes the shear band to initiate sooner than the void does. Also, the average pressure in the cylinder containing the inclusions stays lower than that in the cylinder having similarly situated voids suggesting that the overall stiffness of the cylinder has been reduced more for the rigid inclusion case.

3 Conclusions

We have studied the problem of the initiation and growth of shear bands in a thermally softening viscoplastic cylinder undergoing plane strain deformations. The cylinder has two non-heat-conducting rigid ellipsoidal inclusions, placed on a radial line symmetrically about the center. The complete dynamic thermomechanical problem, including the inertia of the rigid inclusion, has been analyzed. It is found that because of the oscillations of the rigid inclusion, the point where peak values of the maximum principal logarithmic strain occur keeps on changing with time. A shear band initiates from a point close to the left void tip and propagates toward the inner surface. Even though the maximum principal logarithmic strain at a point near the right inclusion tip also increases, these severe deformations stay confined to a very narrow region surrounding the right inclusion tip. Thus, a material point may become unstable in the sense that the effective stress there decreases with increasing strain, but this instability may not propagate farther because either the state of deformation of the material surrounding the inclusion tip is not conducive to that, or the instability is not severe enough.

Acknowledgements

This work was supported by the U.S. Army Research Office grant DAAL 03-91-G-0084 and the U.S. NSF grant MSS 9121279 to the University of Missouri-Rolla. Some of the computations were performed on the NSF sponsored supercomputer center in Ithaca, NY.

References

[1] Batra, R. C., Zhang, X.-T.: Shear band development in dynamic loading of a viscoplastic cylinder containing two voids. Acta Mech. **85,** 221 – 234 (1990).
[2] Zhu, Z. G., Batra, R. C.: Dynamic shear band development in plane strain compression of a viscoplastic body containing a rigid inclusion. Acta Mech. **84,** 89 – 107 (1990).
[3] Batra, R. C., Kim, C. H.: Effect of viscoplastic flow rules on the initiation and growth of shear bands at high strain rates. J. Mech. Phys. Solids **38,** 859 – 874 (1990).

Authors' address: R. C. Batra and X.-T. Zhang, Department of Mechanical and Aerospace Engineering and Engineering Mechanics, University of Missouri-Rolla, Rolla, MO 65401-0249, U.S.A.